frontiers | Frontiers in Physiology

TYPE Original Research
PUBLISHED 21 December 2023
DOI 10.3389/fphys.2023.1284673

OPEN ACCESS

EDITED BY
Hiroshi Matsuura,
Shiga University of Medical Science, Japan

REVIEWED BY
Yosuke Okamoto,
Akita University, Japan
Futoshi Toyoda,
Shiga University of Medical Science, Japan

*CORRESPONDENCE
Hongmei Ruan,
hongmei.ruan@ucsf.edu Vasanth Vedantham,
vasanth.vedantham@ucsf.edu

†PRESENT ADDRESS
Namita Ravi,
Department of Medicine, Brigham and Women's Hospital, Boston MA, United States

‡These authors have contributed equally to this work and share senior authorship

RECEIVED 28 August 2023
ACCEPTED 08 December 2023
PUBLISHED 21 December 2023

CITATION
Ruan H, Mandla R, Ravi N, Galang G, Soe AW, Olgin JE, Lang D and Vedantham V (2023), Cholecystokinin-A signaling regulates automaticity of pacemaker cardiomyocytes. *Front. Physiol.* 14:1284673. doi: 10.3389/fphys.2023.1284673

Cholecystokinin-A signaling regulates automaticity of pacemaker cardiomyocytes

Hongmei Ruan*‡, Ravi Mandla, Namita Ravi†, Giselle Galang, Amanda W. Soe, Jeffrey E. Olgin, Di Lang and Vasanth Vedantham*‡

Cardiology Division, Department of Medicine and Cardiovascular Research Institute, University of California, San Francisco, San Francisco, CA, United States

Aims: The behavior of pacemaker cardiomyocytes (PCs) in the sinoatrial node (SAN) is modulated by neurohormonal and paracrine factors, many of which signal through G-protein coupled receptors (GPCRs). The aims of the present study are to catalog GPCRs that are differentially expressed in the mammalian SAN and to define the acute physiological consequences of activating the cholecystokinin-A signaling system in isolated PCs.

Methods and results: Using bulk and single cell RNA sequencing datasets, we identify a set of GPCRs that are differentially expressed between SAN and right atrial tissue, including several whose roles in PCs and in the SAN have not been thoroughly characterized. Focusing on one such GPCR, Cholecystokinin-A receptor (CCK_AR), we demonstrate expression of *Cckar* mRNA specifically in mouse PCs, and further demonstrate that subsets of SAN fibroblasts and neurons within the cardiac intrinsic nervous system express cholecystokinin, the ligand for CCK_AR. Using mouse models, we find that while baseline SAN function is not dramatically affected by loss of CCK_AR, the firing rate of individual PCs is slowed by exposure to sulfated cholecystokinin-8 (sCCK-8), the high affinity ligand for CCK_AR. The effect of sCCK-8 on firing rate is mediated by reduction in the rate of spontaneous phase 4 depolarization of PCs and is mitigated by activation of beta-adrenergic signaling.

Conclusion: (1) PCs express many GPCRs whose specific roles in SAN function have not been characterized, (2) Activation of the cholecystokinin-A signaling pathway regulates PC automaticity.

KEYWORDS

cholecystokinin, sinoatrial node, pacemaker cell automaticity, GPCR (G protein coupled receptor), cardiac nervous system

1 Introduction

The sinoatrial node (SAN) contains an electrotonically coupled network of pacemaker cardiomyocytes (PCs) that depolarizes the atrial myocardium to initiate the heartbeat. Cellular automaticity in PCs is driven by mutual entrainment of hyperpolarization-activated cyclic nucleotide gated ion channels ("membrane clock") and spontaneous subsarcolemmal calcium release ("calcium clock") (Lakatta et al., 2010). PCs are also densely innervated with sympathetic (Kimura et al., 2012) and post-ganglionic parasympathetic nerve fibers (Rysevaite et al., 2011), the latter originating

within the ganglia of the cardiac intrinsic nervous system (CINS). In addition, paracrine signals from fibroblasts and macrophages, tissue stretch, and humoral input all influence the firing rate of PCs and impulse transmission from the SAN to the atrium. Incorporation of PCs and their complex responses into a patterned network allows the SAN to function as a robust and tunable rhythm generator for the heart.

In this context, it is noteworthy that the complexity of interactions between PCs and their various inputs are only beginning to be unraveled. While the model of mutual antagonism between sympathetic input via norepinephrine and parasympathetic input via acetylcholine explains much SAN behavior, other neurotransmitters and modulators, operating both within the CINS as well as at the CINS-SAN interface, are relevant to SAN function (MacDonald et al., 2020). Supporting the notion of additional pathways relevant to heart rate regulation, recent genome-wide expression studies by our group and other groups have highlighted the enrichment of mRNA encoding several neurotransmitters and neurotransmitter receptors within the CINS and SAN whose specific roles are not well understood, in addition to numerous G-protein coupled receptors (GPCRs) that are differentially expressed in PCs as compared to atrial cardiomyocytes. While physiological roles and functional consequences have been assigned to some of these pathways, many remain uncharacterized.

Here, we survey the landscape of differentially expressed GPCRs in mouse PCs and explore the cholecystokinin signaling pathway, which has not been well characterized in the SAN. In numerous organs and tissues, including the brain and the peripheral nervous system, activation of cholecystokinin A receptor (CCK_AR) by sulfated cholecystokinin octapeptide (sCCK-8), its highest affinity agonist, results in signaling via the heterotrimeric G proteins (typically Gq/11 or Gs) with diverse downstream effects, including induction of gene expression, enzyme secretion, promotion of satiety, natriuresis, and a host of other important physiological consequences (Dufresne et al., 2006). However, much less is known about potential roles for CCK_A signaling in the SAN although its components have been identified in the heart from early stages of cardiac development (Leigh et al., 2021). One prior study found that administration of sCCK-8 to isolated rat hearts results in heart rate slowing that persists despite autonomic blockade (Marker and Roberts, 1988), while a separate study found that low-dose sCCK-8 led to tachycardia in rat hearts while high dose sCCK-8 induced bradycardia (Zhao et al., 2002), suggesting a potentially complex mechanism of action on heart rhythm. However, the possibility of a specific chronotropic effect of cholecystokinin on PCs has not yet been demonstrated.

In the present work, we mine existing mRNA expression datasets to demonstrate that *Cckar* is among the most differentially expressed GPCRs between murine SAN and right atrial cardiomyocytes (Vedantham et al., 2015). We further explore scRNA-seq datasets to define the specific SAN cell populations that express *Cckar* and its ligand, CCK. We then use electrocardiography in WT and $Cckar^{-/-}$ mice and cellular electrophysiology studies in isolated WT and $Cckar^{-/-}$ PCs to explore the potential for CCK_AR signaling to regulate mouse SAN automaticity. Taken together, our data demonstrate a novel signaling axis between the CINS, SAN fibroblasts, and PCs that can regulate cardiac automaticity.

2 Methods

A detailed methods section is available in the Supplementary Material.

2.1 Animal handling and maintenance

Mouse studies were performed under IACUC-approved protocols at the University of California, San Francisco. In accordance with our protocol, animals were euthanized either by carbon dioxide asphyxiation followed by cervical dislocation, or by induction of deep anesthesia with 5% isoflurane, followed by surgical removal of the heart. $Cckar^{tm1Kpn}$ (hereafter, $Cckar^{-/-}$) mice were generated by Alan Kopin et al. and were obtained from Nirao Shah's lab (Kopin et al., 1999). $Cck^{tm1.1(cre)Zjh}$ (hereafter, Cck^{Cre}) mice were obtained from Jackson Labs. $Gt(ROSA)26Sor^{tm4(ACTB-tdTomato,-EGFP)Luo}$ (hereafter, $ROSA^{mT/mG}$) mice were generated by Muzumdar et al. and were obtained from Brian Black's lab (Muzumdar et al., 2007).

2.2 Analysis of gene expression

Bulk RNA sequencing data was generated by Vedantham et al. (2015) and Galang et al. (2020) and downloaded from the Gene Expression Omnibus (GEO, GSE65658 and GSE148515, respectively), while mouse E16.5 SAN single-cell RNA-sequencing data were generated by Goodyer et al. (2019) and downloaded from GEO (GSE132658). Adult rabbit single-cell RNA-seq data were generated by Liang et al. (2021) and were downloaded as fastq files from the NCBI Sequence Read Archive (PRJNA531288). Quantitative PCR was performed using Taqman Probes (Thermo Fisher) with GAPDH as an endogenous control using the ΔΔCT method for comparison of SAN and right atrial tissue. Immunostaining and acetylcholinesterase staining were performed as previously described and are detailed in the Supplementary Methods.

2.3 Transmitter implantation and analysis of heart rhythm data

Adult mice (8–12 weeks old) underwent subcutaneous implantation of telemetry devices (ETA-F10, Data Science International, MN) using 2% inhaled isoflurane for anesthesia according to the manufacturer's instructions. Heart rhythm analysis was performed offline using Ponemah (Data Sciences International, St Paul, MN). 48 h of heart rhythm data were analyzed for each mouse. Time-domain, frequency-domain, and arrhythmia analysis were performed as previously described (Fenske et al., 2016) with modifications detailed in the Supplementary Methods.

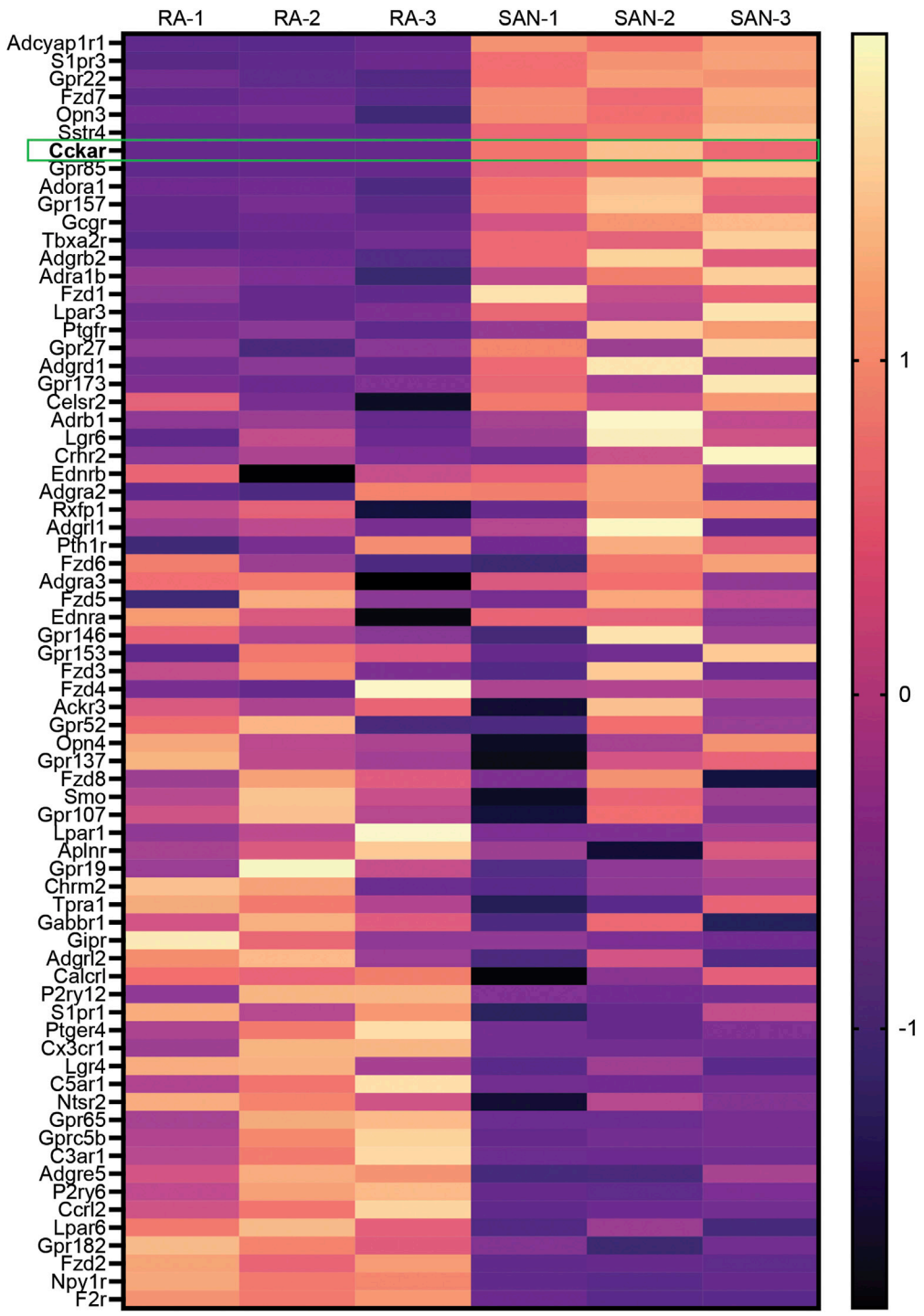

FIGURE 1
Differential Expression of GPCRs in Mammalian Sinoatrial Node. Heatmap demonstrates differentially expressed GPCRs from a previously published dataset 1 with 3 biological replicates of right atrial (RA) cardiomyocytes and sinoatrial node (SAN) pacemaker cardiomyocytes. Color scale indicates z-score. *Cckar* is highlighted.

2.4 Whole cell patch clamp

Adult mouse pacemaker cells were isolated for recording as previously described (Galang et al., 2020) and as detailed in the Supplementary Methods. Action potentials were acquired from spontaneously beating adult cells of the indicated genotypes via the perforated patch-clamp technique with an Axopatch-700B amplifier using pCLAMP10.3. The pCLAMP 10.6 Clampfit module and LabChart7 were used for analysis of action potentials (APs) as detailed in the Supplementary Methods.

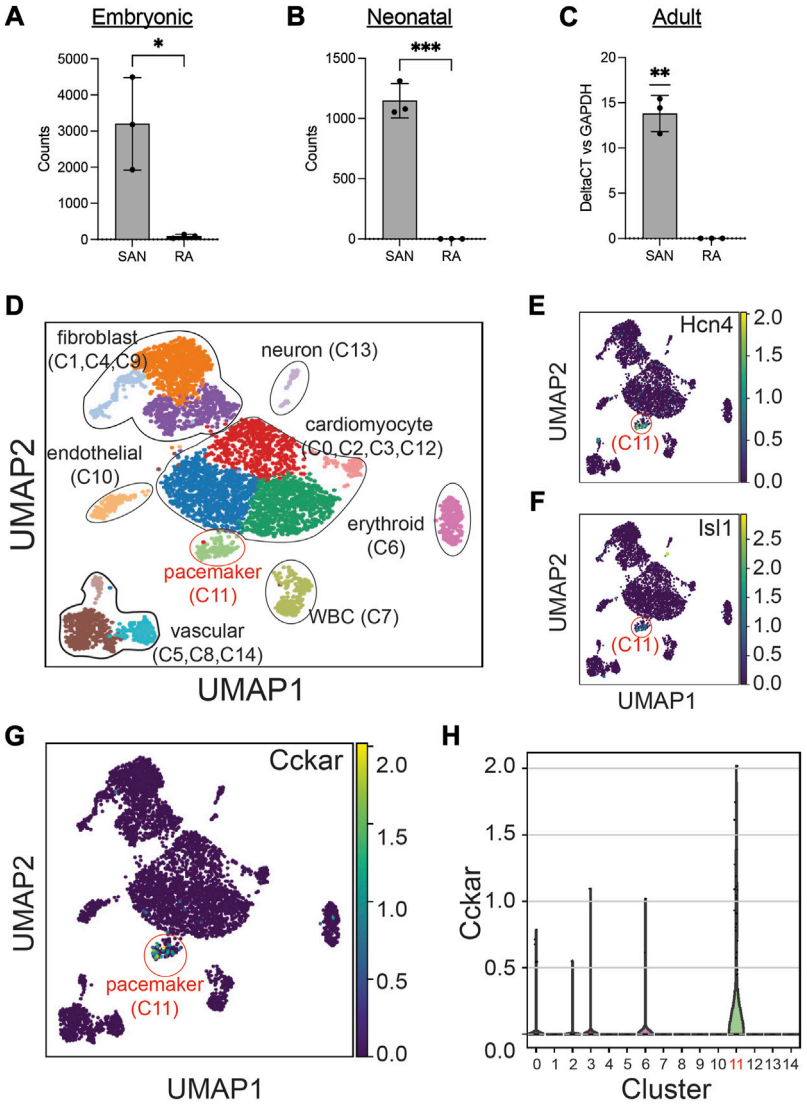

FIGURE 2
Cckar is Expressed in Mouse Cardiac Pacemaker Cells. **(A)** Read counts for Cckar from Bulk RNA sequencing of sinoatrial node (SAN) tissue and right atrial tissue isolated from 3 embryonic day 14.5 Hcn4-GFP BAC transgenic mouse embryos using laser capture microdissection (original dataset from Ref. [9]) A two-tailed *t*-test was used to assess for significance. '*' denotes $p < 0.05$ **(B)** Read counts for *Cckar* from Bulk RNA sequencing of sorted Hcn4-GFP+ pacemaker cells and atrial cardiomyocytes from neonatal mouse hearts shown in the heatmap. A two-tailed *t*-test was used to assess for significance. '***' denotes $p < 0.001$. **(C)** Quantitative PCR for *Cckar* mRNA in samples manually dissected from adult mouse SAN and right atrium, using GAPDH as an endogenous control ($n = 3$ biological replicates). A one-sample *t*-test was used to assess for significance since *Cckar* was not detected in the RA samples. "**" denotes $p < 0.01$ **(D)** Uniform Manifold Approximation Projection (UMAP) plot of leiden clustering analysis of single cell RNA sequencing data derived from 6 E16.5 mouse embryonic heart tissue samples taken from the SAN region demonstrated a pacemaker cell population (red circle, cluster 11), marked by co-expression of *Hcn4* **(E)** and *Isl1* **(F)**, as well as several other identifiable cell types (original dataset from ref [12]). Cckar was differentially expressed in the pacemaker cluster (C11), as seen in the UMAP plot **(G)** and in the violin plot **(H)**.

3 Results

3.1 Differential GPCR expression in the sinoatrial node

To identify GPCRs that might regulate mouse SAN function, we analyzed a previously published bulk RNA sequencing dataset generated by our lab that was derived from sorted neonatal mouse PCs and right atrial cardiomyocytes (RACMs) (Galang et al., 2020). Differentially expressed GPCRs were identified by intersecting the list of expressed genes in both PCs and RACMs with an annotated list of GPCRs obtained from the International Union of Basic and Clinical Pharmacology (Alexander et al., 2019). We identified a total of 71 GPCRs expressed in PCs or RACMs, of which 18 were enriched in RACMs, 13 enriched in the PCs, and 40 expressed in both based on a false discovery rate of 0.05 (Figure 1, Supplementary Table). Among the list of GPCRs highly expressed in PCs were receptors for canonical regulators of SAN function including adenosine (*Adora1*) and norepinephrine (*Adra1b*), as well as some receptors with ligands that do not have established associations with SAN function, such as lysophosphatidic acid (*Lpar3*) and phoenixin (*Gpr173*), orphan GPCRs (*Gpr22*, *Gpr85*,

Gpr157, and *Gpr27*), adhesion GPCRs (*Adgrb2, Adgrd1*), and an opsin (Opn3). A third category of GPCRs included those whose ligands are known to affect SAN function but via mechanisms that have not been fully characterized. This group includes receptors for ligands that are reported to acutely increase heart rate such as glucagon (*Gcgr*) (Mukharji et al., 2013), pituitary adenylate cyclase activating polypeptide (*Adcyap1r1*) (Hoover et al., 2013), prostaglandin $F_{2\alpha}$ (*Ptgfr*) (Courtney et al., 1978), and thromboxane A2 (*Tbx2ar*) (Takayama et al., 2005); receptors whose ligands are reported to acutely decrease heart rate including sphingosine 1-phosphate (*S1pr3*) (Guo et al., 1999) and somatostatin (*Sstr4*) (Bubinski et al., 1993), and one ligand for a highly expressed GPCR for which there exists prior conflicting data on acute physiological responses, cholecystokinin (*Cckar*). Given the unclear effects of cholecystokinin-A signaling in the PCs, and its high degree of differential expression with RACMs, we sought to define the role of this signaling pathway in more detail.

3.2 Cckar and other GPCRs are expressed in sinoatrial node pacemaker cells

To define the expression pattern of *Cckar* in the SAN at different time points, we explored publicly available RNAseq datasets of adult and embryonic SAN tissue. When the SAN was micro-dissected using laser capture (Vedantham et al., 2015), *Cckar* mRNA was highly enriched in SAN compared to right atrial tissue at embryonic day (E)14.5 (Figure 2A). Additional RNA sequencing datasets derived from sorted cells enriched for pacemaker cells (Galang et al., 2020) also confirmed expression of *Cckar* in late embryonic and neonatal murine SAN (Figure 2B). To test whether *Cckar* is expressed in adult SAN tissue, SAN tissue and right atrial tissue were dissected from three 8-week-old adult hearts and *Cckar* mRNA was quantified using GAPDH as an endogenous control. *Cckar* mRNA was detected in all SAN samples but in none of the RA samples (Figure 2C).

The SAN contains pacemaker cells, atrial cardiomyocytes, fibroblasts, and other cell types, so to establish whether *Cckar* expression is restricted to pacemaker cells or is also expressed in other SAN cell populations, we explored recently published single cell RNA sequencing datasets derived from murine and rabbit sinoatrial node. Datasets were clustered using Uniform Manifold Approximation and Projection (Becht et al., 2018) (UMAP) and cell populations identified by expression of established marker genes (Figure 2D). A pacemaker cell cluster was identified that co-expressed *Hcn4* and *Isl1* (Figures 2E, F). Examination of *Cckar* expression within the *Hcn4*$^+$/*Isl1*$^+$ pacemaker cell cluster revealed high and differential expression as compared to other cell types. (Figures 2G, H and Supplementary Figure S1), confirming the presence of *Cckar* transcript specifically in mouse and rabbit cardiac pacemaker cells.

3.3 CCK-expressing neurons and fibroblasts are present in the SAN

Because CCK is produced by many cell types and can function via endocrine signaling pathways as well as via neurotransmission, we hypothesized that sCCK-8 might be produced within the cells of the cardiac intrinsic nervous system that project to the SAN or in other cardiac cell types near pacemaker cells. The scRNA-seq datasets described above demonstrated that *Cck* transcript was observed in both SAN fibroblasts and within a subset of cardiac neurons lying close to the SAN (Figures 3A, B). To test further whether we could observe evidence of *Cck* expression in these cell types, we crossed *Cck*^{cre} mice, in which *Cre recombinase* is inserted downstream of the endogenous *Cck* gene using an internal ribosomal entry site, with *ROSA*^{mTmG} reporter mice, in which membrane targeted GFP is expressed upon recombination by Cre. Thus, GFP$^+$ cells in *CCK-cre; ROSA*^{mTmG} represent cells that have expressed *Cck* for sufficient duration and in sufficient quantity to recombine a reporter allele at the *ROSA* locus.

Consecutive frozen sections from 1 month old *Cck*^{cre}*; ROSA*^{mTmG} hearts were visualized under direct fluorescence and stained with acetyl cholinesterase (AChE), a marker for ganglionated plexi (Figure 3C). Adjacent sections demonstrated GFP+ neurons within the right atrial ganglionated plexus (Figures 3D, E). In addition, GFP+ cellular projections were observed to course within the SAN, visualized by Hcn4 staining (white) and the presence of the SAN artery (denoted by the asterisk), but did not overlap with Hcn4 expression, a marker of cardiac pacemaker cells (Figures 3F–H). The morphology and locations of these projections suggest neuronal identity. In addition to these projections, we also observed several Hcn4$^-$ non-myocyte cells that expressed GFP, with morphologies consistent with fibroblasts (Figures 3I–K). Taken together, the imaging and scRNA-seq data support the conclusions that CCK-producing neurons are present within the heart and project to the SAN and that the SAN contains CCK-expressing fibroblasts. Importantly, these data establish that either the CINS or native SAN fibroblasts (or both) could serve as sources of ligand for Cckar expressed on cardiac pacemaker cells.

3.4 Sinoatrial node function in *Cckar*$^{-/-}$ mice

To test whether CCK_AR is required for SAN function, we assessed heart rhythm and activity using implanted transmitters in *Cckar*$^{-/-}$ mice (n = 11, 8 male and 3 female) in comparison with WT littermates (n = 7, 5 male and 2 female). EKG tracings from both groups of mice were similar with no significant differences in average PR or QRS intervals (Figure 4A, Supplementary Figures S2A–E). With respect to heart rate, the *Cckar*$^{-/-}$ mice exhibited a modest slowing of average heart rate, particularly during waking hours (high activity period) (Figure 4B). Notably, activity counts were also reduced in the *Cckar*$^{-/-}$ mice during similar periods. (Figure 4C). Both intrinsic heart rate (determined after administration of atropine and propranolol under anesthesia) and maximum heart rate (determined after isoproterenol infusion in awake mice) were similar between *Cckar*$^{-/-}$ mice and WT littermates (Figures 4D, E). When heart rate was collated into 10 beat-per-minute bins and plotted in a histogram, there was a modest shift to slightly slower heart rates during high activity periods in the knockout mice, in keeping with their reduced activity counts during these periods (Figure 4F). For each mouse, we also counted sinus pauses, episodes of sinus bradycardia, and episodes of AV block over 48 h of continuous recording and found

10.3389/fphys.2023.1284673

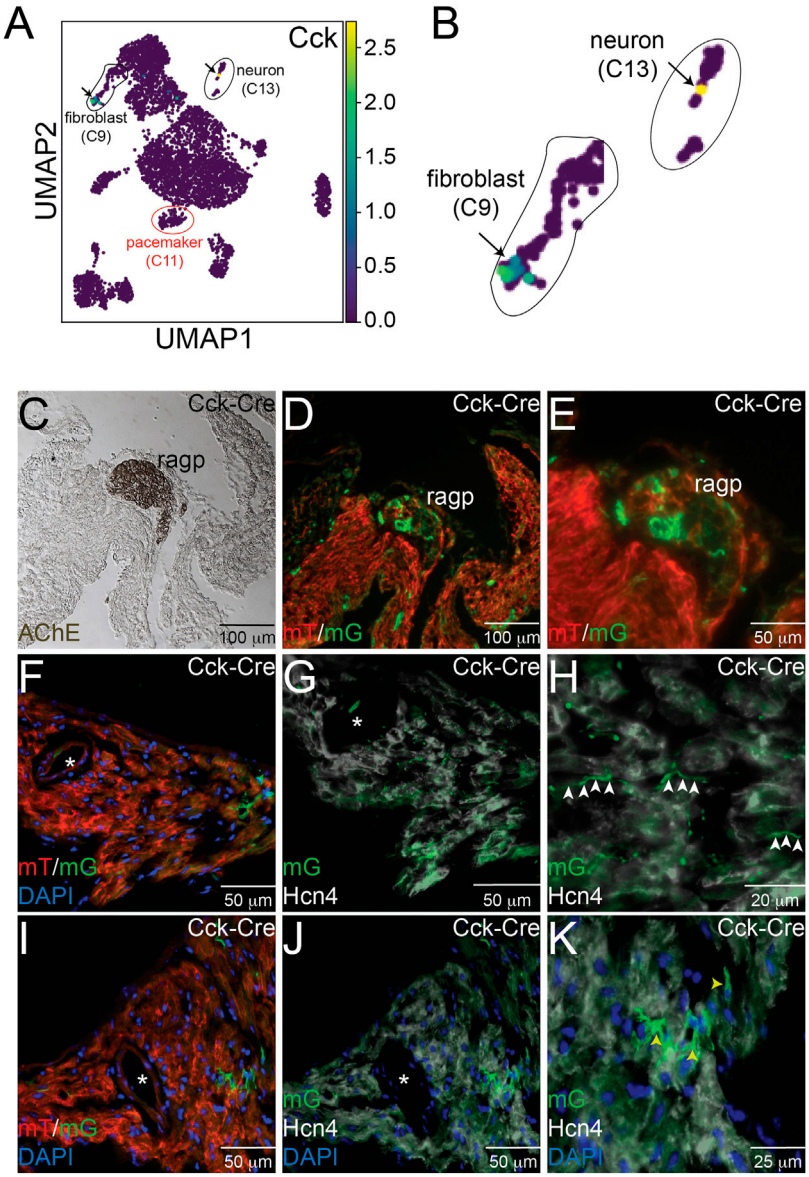

FIGURE 3
Expression of Cck in Neurons and Cardiac Fibroblasts. **(A)** Uniform Manifold Approximation and Projection (UMAP) plot of a single cell RNA sequencing dataset from neonatal sinoatrial node (SAN) (Ref [12]) demonstrates expression of *Cck* in a population of fibroblasts and in a cardiac neuron, as seen in the magnified images in panel **(B)**. Adjacent serial sections from a neonatal *Cck-Cre;ROSA*^{mTmG} mouse heart stained with acetylcholinesterase to mark the right atrial cardiac ganglion **(C)** or imaged with epifluorescence to visualize Td-tomato and GFP expression **(D, E)** demonstrate that GFP+ cells, representing Cck expressing cells, are detectable in neuronal cell bodies within the ganglia. Sectioning and epifluorescence visualization of the SAN *Cck-Cre;ROSA*^{mTmG} showed few GFP+ cells **(F)** but as shown in **(G)** and **(H)**, GFP+ axons could be observed coursing alongside Hcn4+ pacemaker cells (white arrowheads). Notably, GFP expression did not overlap with Hcn4 expression. A nearby section from the SAN **(I)** also revealed GFP+ cells with fibroblast morphologies in the SAN that did not express Hcn4 **(J, K)** – yellow arrowheads). "*" denotes the sinoatrial node artery.

no significant differences in arrhythmia frequency between WT and *Cckar*$^{-/-}$ mice (Supplementary Figures S2F–H). We also assessed heart rate variability in *Cckar*$^{-/-}$ mice in the time domain by estimating the root mean square of successive differences (RMSSD), standard deviation of the RR interval (SDRR), and the percentage of RR intervals differing from the preceding RR interval by 6 msec or more (pNN6) during low activity periods and did not observe any significant differences between the two groups of mice (Supplementary Figures S3A–F). Frequency domain analysis revealed a small increase in low frequency power in *Cckar*$^{-/-}$ mice without significant differences in total power or in high frequency contributions to the power spectra (Supplementary Figures S3G–J).

3.5 sCCK-8 slows spontaneous firing in isolated adult PCs

To test whether signaling via CCK_AR affects electrophysiological properties of PCs, we isolated PCs from adult WT or *Cckar*$^{-/-}$ mice

10.3389/fphys.2023.1284673

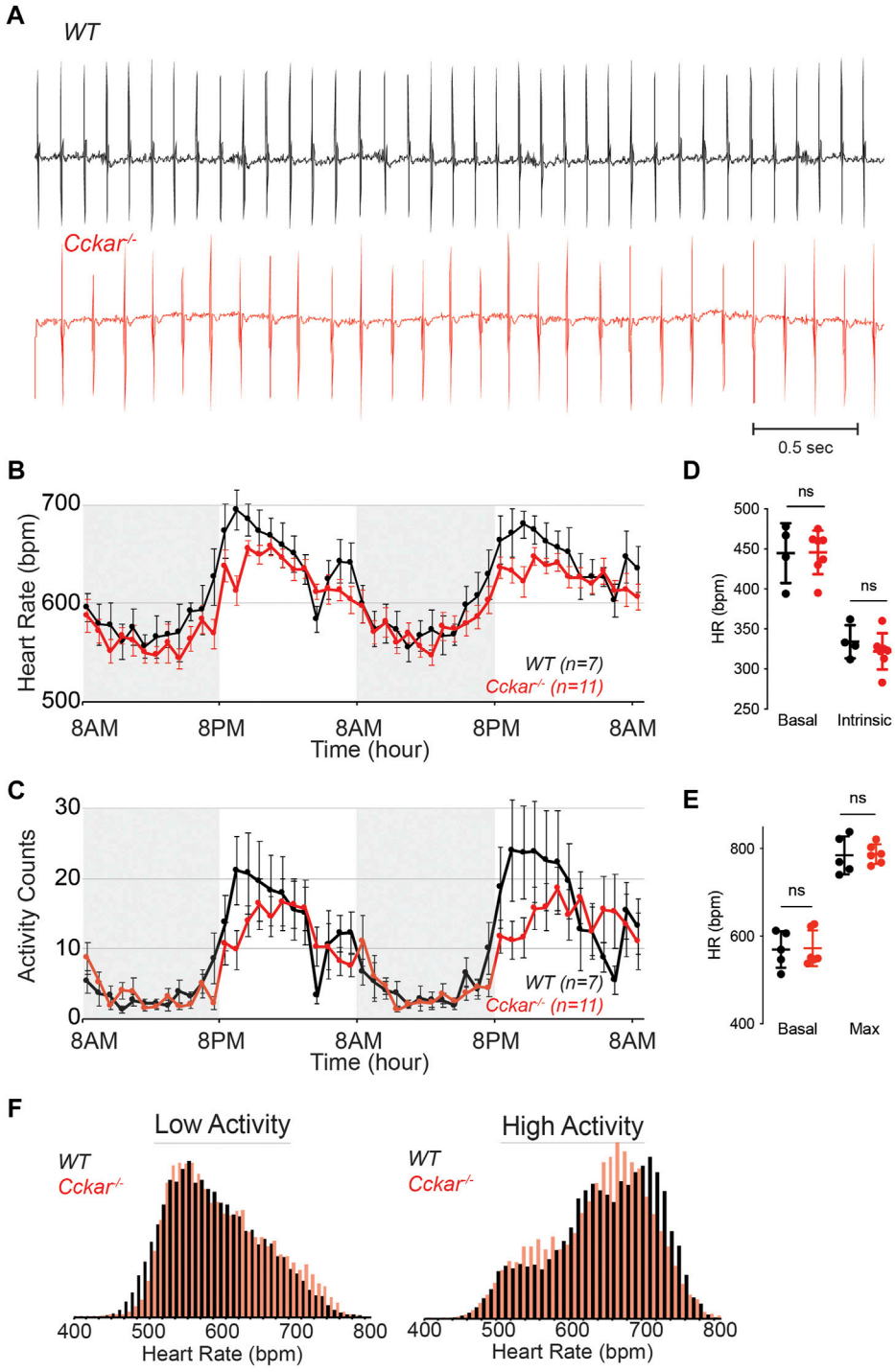

FIGURE 4
Heart Rhythm in *Cckar*$^{-/-}$ Mice. **(A)** Electrocardiographic (ECG) tracings from awake unrestrained WT (top, black) and *Cckar*$^{-/-}$ (bottom, red) adult mice. **(B)** Diurnal heart rate variation among 7 WT and 11 *Cckar*$^{-/-}$adult mice implanted with ECG transmitters. Each point shows mean±SEM. **(C)** Activity counts for 7 WT and 11 *Cckar*$^{-/-}$adult mice implanted with transmitters. Each point shows mean±SEM. **(D)** Heart rate before (baseline) and after atropine and propranolol injection (A/P) in 4 WT (black) and 7 *Cckar*$^{-/-}$mice (red) under anesthesia. Error bars denote standard deviation. **(E)** Heart rate before (baseline) and after isoproterenol injection (Max) in 5 WT (black) and 6 *Cckar*$^{-/-}$ mice (red). Error bars denote standard deviation. A Mann-Whitney test was used to test for significance with $p < 0.05$ deemed significant. 'ns' denotes non-significant. **(F)** Averaged histograms of heart rate during low activity period (left) and high activity period (right) in 7 WT (black) and 11 *Cckar*$^{-/-}$mice (red) with 10 beat per minute bins.

and measured action potentials in whole cell current clamp mode using the perforated patch technique. Individual spontaneously beating mouse pacemaker cells were exposed to sCCK-8, the highest affinity and most widely studied ligand for CCK_AR, at concentrations ranging from 10 pM to 5 nM during AP recording. Whereas there was no acute response of PC firing rate

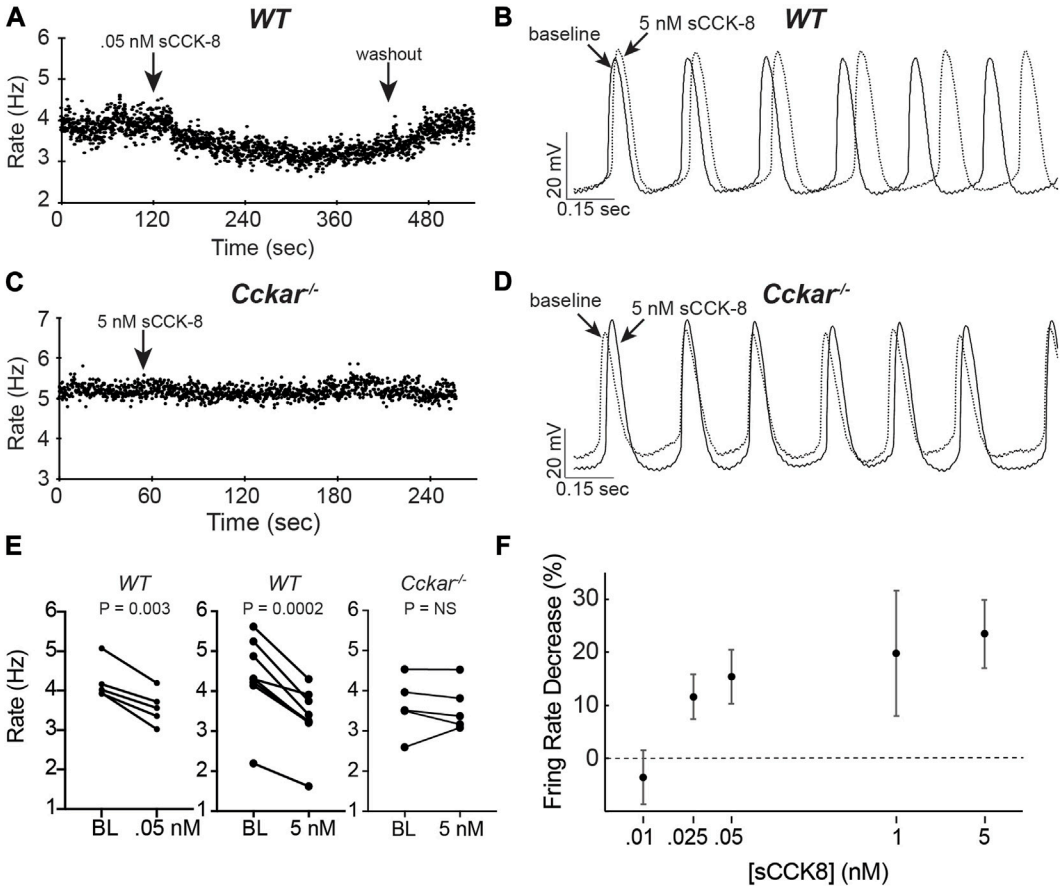

FIGURE 5
sCCK-8 Reduces Spontaneous Firing Rate of Pacemaker Cells. **(A)** Spontaneous firing rate for an isolated adult WT pacemaker cell (PC) before, during perfusion of 50 pM sCCK-8, and after washout. **(B)** Superimposed spontaneous action potentials from an adult WT pacemaker cell firing spontaneously at baseline (solid line) and after perfusion with 5 nM sCCK-8 (dashed line). **(C)** Spontaneous firing rate for an isolated adult *Cckar*$^{-/-}$ pacemaker cell before and during perfusion with 5 nM sCCK-8. **(D)** Superimposed spontaneous action potentials from an adult *Cckar*$^{-/-}$ pacemaker cell at baseline (solid line) and during perfusion with 5 nM sCCK-8 (dashed line). **(E)** Change in spontaneous firing rate of WT PCs at baseline (BL) and after perfusion of 50 nM sCCK-8 (n = 5, left panel) or 5 nM sCCK-8 (n = 8, middle panel) compared with *Cckar*$^{-/-}$ PCs exposed to 5 nM sCCK-8 (n = 5, right panel). Statistical comparison was made with a paired t-test with the indicated p values ("NS" denotes non-significant). **(F)** Percent changein spontaneous firing rate for isolated WT pacemaker cells 1 min after perfusion of 10 pM (n = 3), 25 pM (n = 4), 50 pM (n = 5), 1 nM (n = 7), or 5 nM (n = 8) sCCK-8. Error bars denote standard deviation. Percent change was calculated as 100 x [(R_{BL}−R_{sCCK-8})/R_{BL}], where 'R_{BL}' denotes rate at baseline and 'R_{sCCK-8}' denotes rate after perfusion of sCCK-8.

to perfusion of 10 pM sCCK-8, we observed a dose-dependent reduction in firing rate beginning at 25 pM and reaching a maximal effect of 20%–25% reduction in rate at 1 nM. A dose of 50 pM reached slightly more than half of the maximal effect (Figures 5A, B). The effect on firing rate occurred within 3 min and could be completely washed out at lower concentrations (up to 50 pM) (Figure 5A) but not at 1 nM or above. Importantly, whereas all WT cells examined responded to sCCK-8, none of the PCs isolated from *Cckar*$^{-/-}$ mice responded to the ligand, demonstrating that the physiological effect we observed requires expression of *Cckar* (Figures 5A, C).

To define the electrophysiological mechanism for the reduction in firing rate, AP morphology was quantified before and after exposure of WT and *Cckar*$^{-/-}$ PCs to sCCK-8. Action potential duration at 50% repolarization (APD50, msec), actional potential amplitude (mV), maximum dV/dt (msec/sec), maximum diastolic potential (MDP, mV), takeoff potential (TOP, mV), and early diastolic depolarization (EDDR, mV/msec) were determined at baseline and 2 min after perfusion with 5 nM sCCK-8 (Figure 6A). Notably, there were no significant differences in firing rate or AP morphology between WT and *Cckar*$^{-/-}$ PCs under baseline conditions (Figure 6B). In WT PCs, we observed reductions in EDDR and an increase in APD50 in the presence of sCCK-8, suggesting a signaling mechanism that reduced early spontaneous depolarization and affected repolarization without significantly affecting other components of the pacemaker cell action potential (Figure 6C). Importantly, we did not observe changes in AP morphology in PCs from *Cckar*$^{-/-}$ mice exposed to sCCK-8, again underscoring the dependence of the pharmacological effect on the expression of CCK_AR (Figure 6D).

In PCs, EDDR is largely determined by current through Hcn channels, whose voltage-dependence is sensitive to cyclic adenosine monophosphate (cAMP) concentration (DiFrancesco, 2010). To

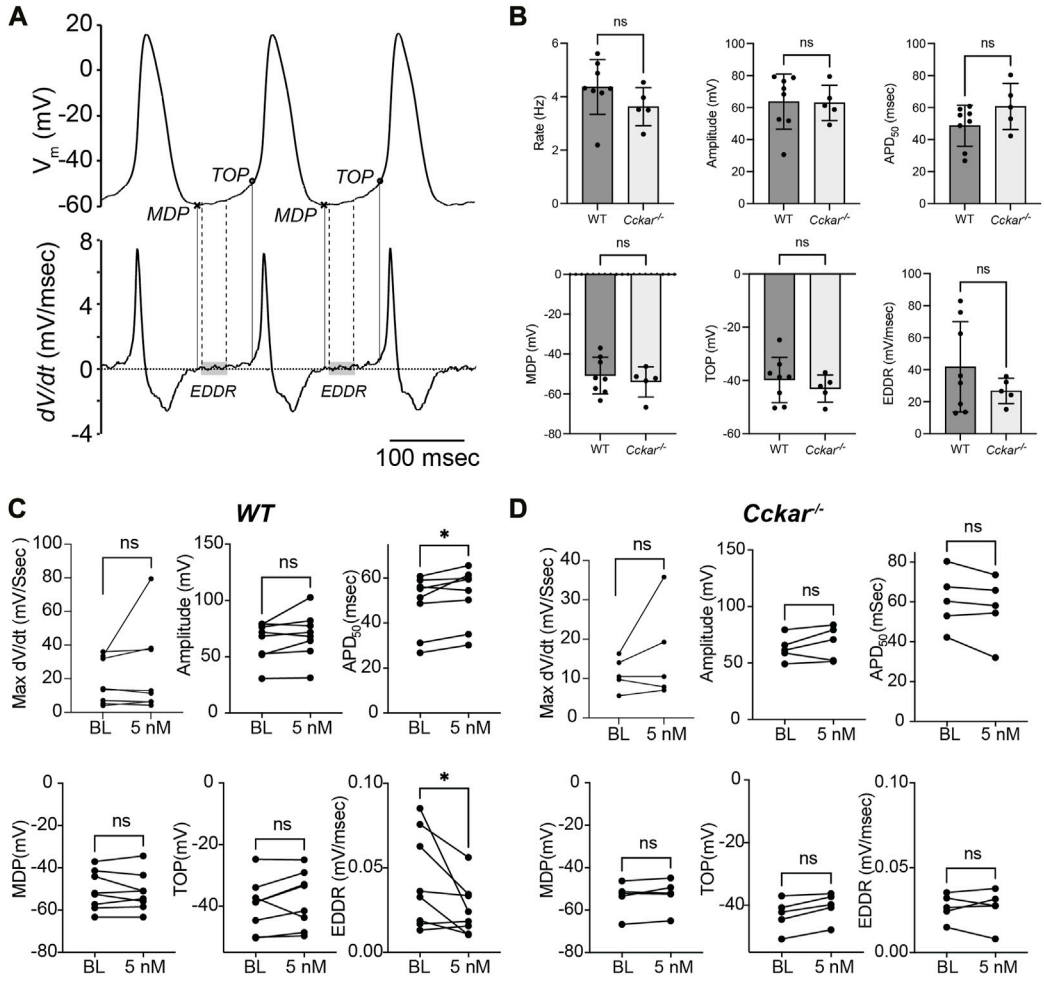

FIGURE 6
sCCK-8 Reduces Early Spontaneous Depolarization in Pacemaker Cardiomyocytes. **(A)**. Definition of action potential parameters. The top tracing, $V_m(t)$, shows spontaneous action potentials (APs) from an isolated adult pacemaker cell and the bottom tracing shows the first derivative (dV/dt). The minimum diastolic potential (MDP) was defined as the minimum potential recorded between action potentials; Take off potential (TOP) was defined as the membrane potential at which dV/dt reach 10% of its maximum value; and early diastolic depolarization rate (EDDR) was defined as the average value of dV/dt over the shaded area in the bottom panel (from 10% to 50% of the MDP-to-TOP interval). **(B)** AP parameters including Firing Rate, Amplitude, APD_{50}, MDP, TOP, and EDDR were measured under baseline conditions in WT and *Cckar*$^{-/-}$ PCs (n = 8 and n = 5, respectively). Measurements of these parameters were also compared before and 3 min after perfusion with 5 nM sCCK-8 for **(C)** WT and **(D)** *Cckar*$^{-/-}$ PCs. Statistical comparisons between baseline values and between pre- and post-sCCK-8 values were made with a Mann-Whitney test ("ns" denotes non-significant, "*" denotes $p < 0.05$).

determine whether the effect of sCCK-8 is independent of this pathway, we tested whether the sCCK-8 induced reduction in firing rate could be fully or partially abrogated by co-administration of 1 nM isoproterenol, a beta-adrenergic agonist that increases cAMP via Gs. In contrast to the robust effect observed in the absence of isoproterenol, in the presence of isoproterenol, perfusion of 1 nM (n = 5) sCCK-8 had no effect on PC firing rate, with some but not all cells exhibiting a partial response at 2.5 nM (n = 7) and 5 nM (n = 6), and all cells exhibiting a partial effect at 10 nM (n = 6) and 20 nM (n = 4) (Supplementary Figure S4). Cells from *Cckar*$^{-/-}$ mice were insensitive to sCCK-8 in the presence of isoproterenol, as expected. Examination of AP morphology demonstrated that in the presence of isoproterenol, there was no significant change in EDDR at 5 nM s-CCK8 though a significant reduction could be observed at 10 nM (Supplementary Figure S5).

4 Discussion

Our main findings are (1) mammalian PCs express functional CCK_AR, (2) CINS neurons and SAN fibroblasts express CCK, and (3) sCCK-8 slows PC firing rate by reducing the slope of early diastolic depolarization. Taken together, these data provide evidence for a novel signaling system in PCs that could affect mammalian SAN function through direct effects on automaticity.

4.1 GPCR expression in the SAN

Analysis of existing RNA sequencing datasets identified several GPCRs that are enriched in SAN tissue and expressed in both SAN and atrial tissue, including orphan GPCRs and GPCRs with defined ligands but no known functions in

regulating heart rhythm. Ligands for several of these GPCRs, including *Sstr4*, *S1pr3*, *Gcgr*, and *Adcyap1r1* trigger defined chronotropic responses but the molecular mechanisms driving their specific actions on isolated pacemaker cells have been characterized only for some (Sanna et al., 2016). Our findings of high-level and differential expression of these receptors in PCs suggest that chronotropic responses to these ligands are mediated by direct effects on PC automaticity. Further work will be required to define the specific electrophysiological effects of these signaling pathways on PCs in physiological contexts and to identify the relevant sources of their ligands. Importantly, leading computational models of the PC action potential have yet to incorporate dynamic signaling through simultaneously activated receptors for these various ligands, and the potential roles of these signaling pathways in long-term versus short-term SAN physiology have not been determined. The catalog of GPCRs presented here could form a foundation for such efforts and for deeper exploration of interaction between the CINS and SAN beyond the canonical signaling pathways involved in autonomic regulation of the heartbeat.

4.2 Expression of cholecystokinin signaling pathway components in the SAN

Recent studies have explored the functional neuroanatomy of the cardiac intrinsic nervous system with particular attention to innervation of the SAN. In a recent single cell qPCR analysis of porcine heart, CCK-expressing neurons were identified as a subset of right atrial ganglionated plexus neurons and included cells that projected directly to the SAN (Moss et al., 2021). Using a Cck^{Cre} mouse line to drive reporter gene expression, we uncovered similar findings in mice, with Cre-expressing neurons observed in the RAGP and in projections within the SAN, findings that we confirmed with analysis of scRNA-seq data. An additional finding of note is the presence of CCK-expressing fibroblasts within the SAN which has not been previously described and raises the possibility of paracrine signaling from SAN fibroblasts to pacemaker cells. Finally, CCK peptides are present in picomolar concentrations in serum, so the possibility of endocrine signaling to the SAN cannot be excluded.

For our experiments, we used sCCK-8, the most commonly studied form of CCK (Wank, 1995)and the isoform that has been used previously to study the role of CCK in the cardiovascular system (Gaw et al., 1995). CCK is synthesized as a 115-amino acid preprohormone (Deschenes et al., 1984), and is then cleaved and processed into several bioactive forms, including CCK-58, CCK-39/33, CCK-8, and CCK-4 (Deschenes et al., 1984). CCK_AR has a reporter affinity for sulfated CCK-8 that is greater than in its affinity for other isoforms, although the C-terminal heptapeptide is the critical portion of the ligand for all forms of CCK (Wu et al., 2008). A key difference between different CCK peptides appears to be pre-receptor handling, such that CCK-8 has a shorter half-life in serum than the longer isoforms and thus may be more suited to function as a neurotransmitter. Because we focused on sCCK-8 only, our data cannot exclude that possibility that other forms of CCK could have different effects than what we observed. Although further work would be required to establish common and different actions of CCK isoforms on PCs, we note that all bioactive CCK peptides have the same C-terminal heptapeptide and often have similar biological activity in other contexts. Thus, we hypothesize that other forms of CCK would have a broadly similar effect on PCs. However, the stimulus for secretion and whether such signaling might play a role in sinus node dysfunction remain to be determined. However, the deep conservation of expression of the CCK signaling system among mammals suggests a conserved functional role in SAN function and in autonomic regulation of heart rhythm.

4.3 Role of cholecystokinin signaling in regulating heart rhythm

Although $Cckar^{-/-}$ mice had modestly slower heart rates than WT mice during high activity periods, this might have resulted from lower activity levels in these mice owing to the involvement of CCK_AR in many central and peripheral neuronal and organ-specific signaling pathways that affect mouse behavior. Thus, reduced activity in $Cckar^{-/-}$ mice could have led to the slower heart rates, although we cannot exclude the opposite possibility that compromised SAN function reduced activity levels. However, our finding that $Cckar^{-/-}$ mice do not exhibit sinus node dysfunction or changes in intrinsic heart rate after autonomic blockade suggests that CCK_AR signaling is not required for SAN function under baseline conditions in adult mice. Related to this point, the magnitude of the sCCK-8 effect on isolated pacemaker cells is modest as assessed on a short time scale and could be counteracted by co-administration of isoproterenol, suggesting that the primary role of this pathway in autonomic regulation of SAN function may not be direct beat-to-beat regulation of heart rate. Alternatively, there may be redundant mechanisms that mitigate the loss of CCK_AR in $Cckar^{-/-}$mice.

4.4 Acute effects of cckar signaling on isolated pacemaker cells

Previous studies in rodent models have demonstrated that injection of sCCK-8 into an anesthetized animal or bolus injection of sCCK-8 to the heart *ex-vivo* can produce changes in heart rate (Marker and Roberts, 1988; Zhao et al., 2002). Our work extends these findings by demonstrating that sCCK-8 acutely and directly reduces the firing rate of PCs by lowering the EDDR and lengthening the APD. Of note, the 20–50 picomolar EC50 for the effect of sCCK-8 on firing rate is similar to its EC50 for release of amylase from pancreatic acini and corresponds to only partial equilibrium occupancy of the receptor based on radioligand binding assays (Jensen et al., 1980).

Our data support establish that sCCK-8 slows PC firing, but they do not establish the molecular basis for this effect. While CCK_AR is generally considered to signal preferentially via Gq (Liu et al., 2021), signaling via Gs (Wu et al., 1997), Gi (Scemama et al., 1988), or G12/13 (Le Page et al., 2003; Sabbatini et al., 2010) has been reported in different cellular contexts. Of note, activation of Gq specifically in murine SAN PCs using a genetically encoded optogenetic tool *increased* heart rate by

~5% (Wagdi et al., 2021), while activation of Gq using DREADD technology resulted in a non-significant increase in heart rate (Kaiser et al., 2019), suggesting that the acute decrease in firing rate we observed may not result purely from signaling via Gq.

Although not the preferred downstream pathway in most contexts, some considerations support signaling via Gi as a mechanism that could contribute to the pharmacological effects we observed. First, the reduction in EDDR suggests that reduced inward current through Hcn channels may be responsible for the reduction in firing rate (Bucchi et al., 2007). In addition to their established roles in activating G-protein activated inward rectifying currents (GIRK) in the SAN, activation of Gi also reduces cyclic adenosine monophosphate (cAMP) levels and thereby shifts the voltage dependence of Hcn current activation to more positive potentials (Accili et al., 1998). The shift in Hcn voltage dependence reduces the slope of diastolic depolarization, thereby lowering firing rate which is what we observed (Accili et al., 1998). In addition, we found that administration of isoproterenol partially blunted the effect of sCCK-8 on firing rate. Because isoproterenol acts via Gs to increase cAMP concentration, the balance of Gi and Gs activation regulates the availability of cAMP for binding to Hcn channels. Thus, our hypothesis that CCK_AR couples to Gi in the SAN to reduce firing rate would predict that activation of Gs via adrenergic signaling would antagonize the effect, as we observed. Further work with direct inhibition of Gi and Gq in pacemaker cells and measurement of ionic currents before and after sCCK-8 administration will be required to test this hypothesis.

4.5 Limitations

Our study does not directly address the possibility that CCK_AR signaling affects SAN properties not related to acute physiological response. In addition, we used a global loss of function model, which confounds our ability to define the physiological consequences of perturbing CCK_AR signaling specifically in PCs. Despite these limitations, the present study demonstrates functional expression of CCK_AR in PCs and establishes a foundation for future work on this signaling pathway and its relevance to heart rhythm regulation.

Data availability statement

The datasets presented in this study can be found in online repositories. The names of the repository/repositories and accession number(s) can be found in the article/Supplementary Material.

Ethics statement

The animal study was approved by UCSF Institutional Animal Care and Use Committee. The study was conducted in accordance with the local legislation and institutional requirements.

Author contributions

HR: Conceptualization, Investigation, Supervision, Writing–original draft, Writing–review and editing. RM: Data curation, Investigation, Writing–review and editing. NR: Investigation, Writing–review and editing. GG: Investigation, Writing–review and editing. AS: Investigation, Writing–review and editing. JO: Supervision, Writing–review and editing. DL: Investigation, Writing–review and editing. VV: Investigation, Supervision, Writing–original draft, Writing–review and editing.

Funding

The author(s) declare financial support was received for the research, authorship, and/or publication of this article. This work was supported by the National Institutes of Health (grant number DP2HL152425 to VV); the American Heart Association (Career Development Award 846898 to DL); and the Sarnoff Cardiovascular Research Foundation (Research Fellowship to NR).

Acknowledgments

The authors are grateful to Huiliang Qui for assistance with preparing materials for physiology experiments, and to Gagandeep Chouhan for assistance with genotyping and mouse colony management.

Conflict of interest

VV received research grants from Amgen and consulting fees from Merck that were unrelated to the research presented in this manuscript.

The remaining authors declare that the research was conducted in the absence of any commercial or financial relationships that could be construed as a potential conflict of interest.

Publisher's note

Supplementary material

The Supplementary Material for this article can be found online at: https://www.frontiersin.org/articles/10.3389/fphys.2023.1284673/full#supplementary-material

References

Accili, E. A., Redaelli, G., and DiFrancesco, D. (1998). Two distinct pathways of muscarinic current responses in rabbit sino-atrial node myocytes. *Pflugers Arch.* 437, 164–167. doi:10.1007/s004240050763

Alexander, S. P. H., Christopoulos, A., Davenport, A. P., Kelly, E., Mathie, A., Peters, J. A., et al. (2019). The concise guide to pharmacology 2019/20: G protein-coupled receptors. *Br. J. Pharmacol.* 176 (Suppl. 1), S21–S141. doi:10.1111/bph.14748

Becht, E., McInnes, L., Healy, J., Dutertre, C. A., Kwok, I. W. H., Ng, L. G., et al. (2018). Dimensionality reduction for visualizing single-cell data using umap. *Nat. Biotechnol.* 37, 38–44. doi:10.1038/nbt.4314

Bubinski, R., Kus, W., and Goch, J. (1993). Effect of somatostatin on the conduction system of the heart. *Kardiol. Pol.* 38, 258–262.

Bucchi, A., Baruscotti, M., Robinson, R. B., and DiFrancesco, D. (2007). Modulation of rate by autonomic agonists in san cells involves changes in diastolic depolarization and the pacemaker current. *J. Mol. Cell. Cardiol.* 43, 39–48. doi:10.1016/j.yjmcc.2007.04.017

Courtney, K. R., Colwell, W. T., and Jensen, R. A. (1978). Prostaglandins and pacemaker activity in isolated Guinea pig sa node. *Prostaglandins* 16, 451–459. doi:10.1016/0090-6980(78)90224-1

Deschenes, R. J., Lorenz, L. J., Haun, R. S., Roos, B. A., Collier, K. J., and Dixon, J. E. (1984). Cloning and sequence analysis of a cdna encoding rat preprocholecystokinin. *Proc. Natl. Acad. Sci. U. S. A.* 81, 726–730. doi:10.1073/pnas.81.3.726

DiFrancesco, D. (2010). The role of the funny current in pacemaker activity. *Circulation Res.* 106, 434–446. doi:10.1161/CIRCRESAHA.109.208041

Dufresne, M., Seva, C., and Fourmy, D. (2006). Cholecystokinin and gastrin receptors. *Physiol. Rev.* 86, 805–847. doi:10.1152/physrev.00014.2005

Fenske, S., Probstle, R., Auer, F., Hassan, S., Marks, V., Pauza, D. H., et al. (2016). Comprehensive multilevel *in vivo* and *in vitro* analysis of heart rate fluctuations in mice by ecg telemetry and electrophysiology. *Nat. Protoc.* 11, 61–86. doi:10.1038/nprot.2015.139

Galang, G., Mandla, R., Ruan, H., Jung, C., Sinha, T., Stone, N. R., et al. (2020). Atac-seq reveals an isl1 enhancer that regulates sinoatrial node development and function. *Circ. Res.* 127, 1502–1518. doi:10.1161/CIRCRESAHA.120.317145

Gaw, A. J., Hills, D. M., and Spraggs, C. F. (1995). Characterization of the receptors and mechanisms involved in the cardiovascular actions of scck-8 in the pithed rat. *Br. J. Pharmacol.* 115, 660–664. doi:10.1111/j.1476-5381.1995.tb14983.x

Goodyer, W. R., Beyersdorf, B. M., Paik, D. T., Tian, L., Li, G., Buikema, J. W., et al. (2019). Transcriptomic profiling of the developing cardiac conduction system at single-cell resolution. *Circulation Res.* 125, 379–397. doi:10.1161/CIRCRESAHA.118.314578

Guo, J., MacDonell, K. L., and Giles, W. R. (1999). Effects of sphingosine 1-phosphate on pacemaker activity in rabbit sino-atrial node cells. *Pflugers Arch.* 438, 642–648. doi:10.1007/s004249900067

Hoover, D. B., Girard, B. M., Hoover, J. L., and Parsons, R. L. (2013). PAC$_1$ receptors mediate positive chronotropic responses to PACAP-27 and VIP in isolated mouse atria. *Eur. J. Pharmacol.* 713, 25–30. doi:10.1016/j.ejphar.2013.04.037

Jensen, R. T., Lemp, G. F., and Gardner, J. D. (1980). Interaction of cholecystokinin with specific membrane receptors on pancreatic acinar cells. *Proc. Natl. Acad. Sci. U. S. A.* 77, 2079–2083. doi:10.1073/pnas.77.4.2079

Kaiser, E., Tian, Q., Wagner, M., Barth, M., Xian, W., Schroder, L., et al. (2019). Dreadd technology reveals major impact of gq signalling on cardiac electrophysiology. *Cardiovasc Res.* 115, 1052–1066. doi:10.1093/cvr/cvy251

Kimura, K., Ieda, M., and Fukuda, K. (2012). Development, maturation, and transdifferentiation of cardiac sympathetic nerves. *Circ. Res.* 110, 325–336. doi:10.1161/CIRCRESAHA.111.257253

Kopin, A. S., Mathes, W. F., McBride, E. W., Nguyen, M., Al-Haider, W., Schmitz, F., et al. (1999). The cholecystokinin-a receptor mediates inhibition of food intake yet is not essential for the maintenance of body weight. *J. Clin. Investig.* 103, 383–391. doi:10.1172/JCI4901

Lakatta, E. G., Maltsev, V. A., and Vinogradova, T. M. (2010). A coupled system of intracellular ca2+ clocks and surface membrane voltage clocks controls the timekeeping mechanism of the heart's pacemaker. *Circ. Res.* 106, 659–673. doi:10.1161/CIRCRESAHA.109.206078

Leigh, R. S., Ruskoaho, H. J., and Kaynak, B. L. (2021). Cholecystokinin peptide signaling is regulated by a tbx5-mef2 axis in the heart. *Peptides* 136, 170459. doi:10.1016/j.peptides.2020.170459

Le Page, S. L., Bi, Y., and Williams, J. A. (2003). Cck-a receptor activates rhoa through g alpha 12/13 in nih3t3 cells. *Am. J. Physiol. Cell. Physiol.* 285, C1197–C1206. doi:10.1152/ajpcell.00083.2003

Liang, D., Xue, J., Geng, L., Zhou, L., Lv, B., Zeng, Q., et al. (2021). Cellular and molecular landscape of mammalian sinoatrial node revealed by single-cell rna sequencing. *Nat. Commun.* 12, 287. doi:10.1038/s41467-020-20448-x

Liu, Q., Yang, D., Zhuang, Y., Croll, T. I., Cai, X., Dai, A., et al. (2021). Ligand recognition and g-protein coupling selectivity of cholecystokinin a receptor. *Nat. Chem. Biol.* 17, 1238–1244. doi:10.1038/s41589-021-00841-3

MacDonald, E. A., Rose, R. A., and Quinn, T. A. (2020). Neurohumoral control of sinoatrial node activity and heart rate: insight from experimental models and findings from humans. *Front. Physiol.* 11, 170. doi:10.3389/fphys.2020.00170

Marker, J. D., and Roberts, M. L. (1988). Chronotropic actions of cholecystokinin octapeptide on the rat heart. *Regul. Pept.* 20, 251–259. doi:10.1016/0167-0115(88)90081-x

Moss, A., Robbins, S., Achanta, S., Kuttippurathu, L., Turick, S., Nieves, S., et al. (2021). A single cell transcriptomics map of paracrine networks in the intrinsic cardiac nervous system. *iScience* 24, 102713. doi:10.1016/j.isci.2021.102713

Mukharji, A., Drucker, D. J., Charron, M. J., and Swoap, S. J. (2013). Oxyntomodulin increases intrinsic heart rate through the glucagon receptor. *Physiol. Rep.* 1, e00112. doi:10.1002/phy2.112

Muzumdar, M. D., Tasic, B., Miyamichi, K., Li, L., and Luo, L. (2007). A global double-fluorescent cre reporter mouse. *Genesis* 45, 593–605. doi:10.1002/dvg.20335

Rysevaite, K., Saburkina, I., Pauziene, N., Noujaim, S. F., Jalife, J., and Pauza, D. H. (2011). Morphologic pattern of the intrinsic ganglionated nerve plexus in mouse heart. *Heart rhythm.* 8, 448–454. doi:10.1016/j.hrthm.2010.11.019

Sabbatini, M. E., Bi, Y., Ji, B., Ernst, S. A., and Williams, J. A. (2010). Cck activates rhoa and rac1 differentially through galpha13 and galphaq in mouse pancreatic acini. *Am. J. Physiol. Cell. Physiol.* 298, C592–C601. doi:10.1152/ajpcell.00448.2009

Sanna, M. G., Vincent, K. P., Repetto, E., Nguyen, N., Brown, S. J., Abgaryan, L., et al. (2016). Bitopic sphingosine 1-phosphate receptor 3 (s1p3) antagonist rescue from complete heart block: pharmacological and genetic evidence for direct s1p3 regulation of mouse cardiac conduction. *Mol. Pharmacol.* 89, 176–186. doi:10.1124/mol.115.100222

Scemama, J. L., Robberecht, P., Waelbroeck, M., De Neef, P., Pradayrol, L., Vaysse, N., et al. (1988). Cck and gastrin inhibit adenylate cyclase activity through a pertussis toxin-sensitive mechanism in the tumoral rat pancreatic acinar cell line ar 4-2j. *FEBS Lett.* 242, 61–64. doi:10.1016/0014-5793(88)80985-2

Takayama, K., Yuhki, K., Ono, K., Fujino, T., Hara, A., Yamada, T., et al. (2005). Thromboxane a2 and prostaglandin f2alpha mediate inflammatory tachycardia. *Nat. Med.* 11, 562–566. doi:10.1038/nm1231

Vedantham, V., Galang, G., Evangelista, M., Deo, R. C., and Srivastava, D. (2015). Rna sequencing of mouse sinoatrial node reveals an upstream regulatory role for islet-1 in cardiac pacemaker cells. *Circulation Res.* 116, 797–803. doi:10.1161/CIRCRESAHA.116.305913

Wagdi, A., Malan, D., Beauchamp, J. S., Naryanan, U. B. S., Dusend, V., Sasse, P., et al. (2021). Opn5 a new optogenetic receptor to study gq signalling in the heart with light. *EP Eur.* 23, 574. doi:10.1093/europace/euab116.574

Wank, S. A. (1995). Cholecystokinin receptors. *Am. J. Physiol.* 269, G628–G646. doi:10.1152/ajpgi.1995.269.5.G628

Wu, S. V., Harikumar, K. G., Burgess, R. J., Reeve, J. R., Jr., and Miller, L. J. (2008). Effects of cholecystokinin-58 on type 1 cholecystokinin receptor function and regulation. *Am. J. Physiol. Gastrointest. Liver Physiol.* 295, G641–G647. doi:10.1152/ajpgi.90390.2008

Wu, V., Yang, M., McRoberts, J. A., Ren, J., Seensalu, R., Zeng, N., et al. (1997). First intracellular loop of the human cholecystokinin-a receptor is essential for cyclic amp signaling in transfected hek-293 cells. *J. Biol. Chem.* 272, 9037–9042. doi:10.1074/jbc.272.14.9037

Zhao, X. Y., Ling, Y. L., Meng, A. H., Shan, B. E., and Zhang, J. L. (2002). Effects of cholecystokinin octapeptide on rat cardiac function and the receptor mechanism. *Sheng Li Xue Bao* 54, 239–243.